

The post-perovskite transition in Fe- and Al-bearing bridgmanite

Juan J. Valencia-Cardona¹, Jingyi Zhuang², Renata M. Wentzcovitch^{2,3},
Gaurav Shukla⁴, Kanchan Sarkar^{2,3}

1. Logic Technology Development, Intel Corporation, Hillsboro, OR
2. Columbia University, Department of Applied Physics and Applied Mathematics, NY
3. Columbia University, Lamont-Doherty Earth Observatory, Palisades
4. Indian Institute of Science Education and Research Kolkata, Department of Earth Sciences, Mohanpur, West Bengal, India



Abstract

The major phase of the Earth's mantle, (Al,Fe)-bearing bridgmanite, transitions to the post-perovskite (PPv) phase at Earth's deep lower mantle conditions. Despite extensive experimental and ab initio investigations, there are still important aspects of this transformation that need clarification. Here, we address this transition in (Al³⁺, Fe³⁺)-, (Al³⁺)-, (Fe²⁺)- and (Fe³⁺)-bearing bridgmanite using ab initio calculations. We find that the seismic features produced by the PPv transition depend distinctly on the chemical composition. For instance, Fe³⁺-, Al³⁺-, or (Al³⁺, Fe³⁺)-alloying increase the transition pressure, while Fe²⁺-alloying has the opposite effect. Consequently, the absence of a D'' seismic discontinuity or signature of a double-crossing of the PPv phase boundary point to a Fe²⁺-poor and Fe³⁺-rich bridgmanite composition with profound implications for the redox state of the deep lower mantle. These chemistry-specific seismic features together, along with thermochemical equilibrium calculations will be fundamental for resolving the chemical composition of the D'' region by direct inspection of tomographic images.

Methods and calculation details

- Bridgmanites, post-perovskites by Shukla et al. [1,2,3]
- Quantum ESPRESSO software [4]
- LDA + U_{sc}, GGA + U_{sc}, 40-atom supercells
- Quasi-harmonic approximation

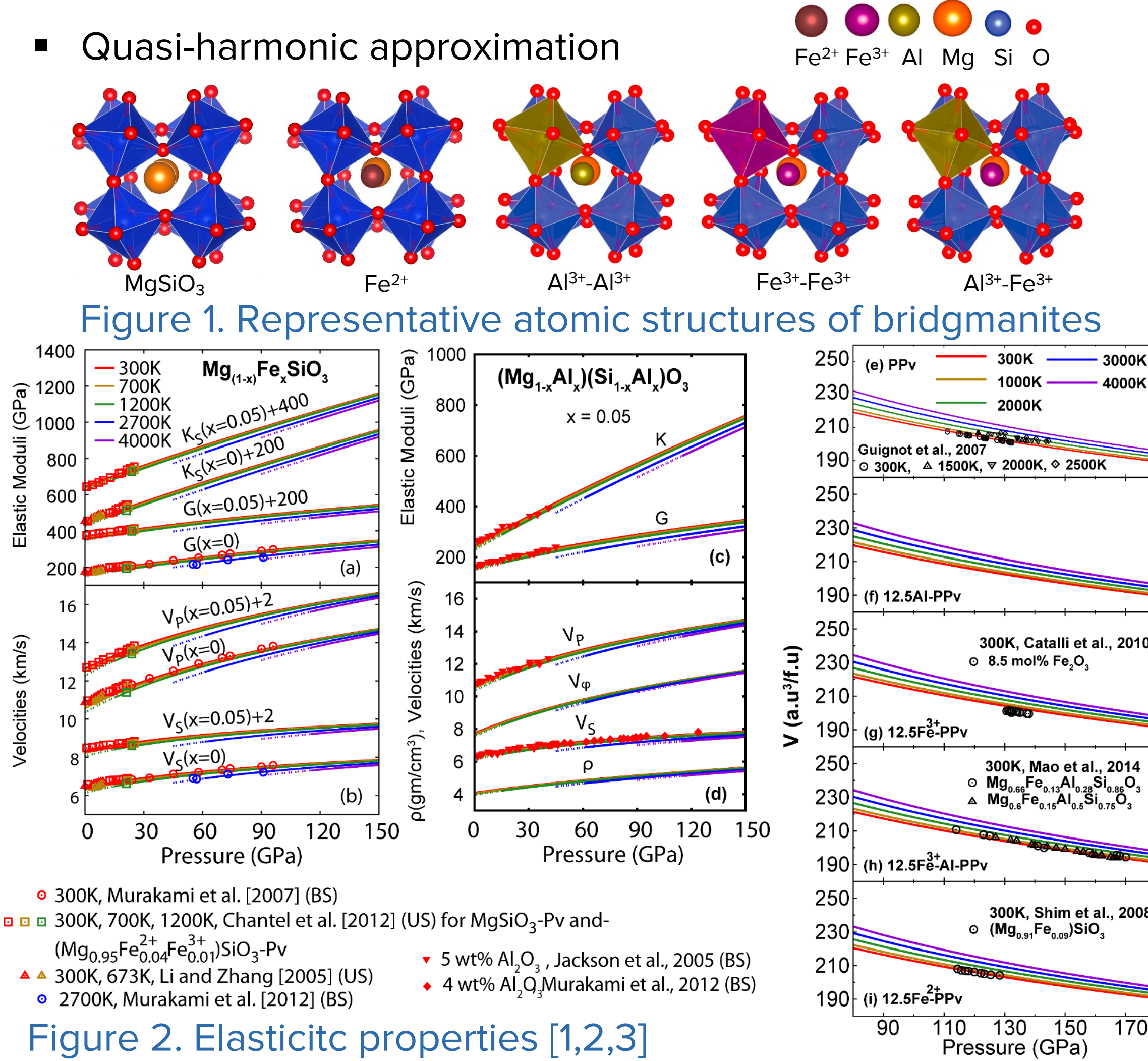
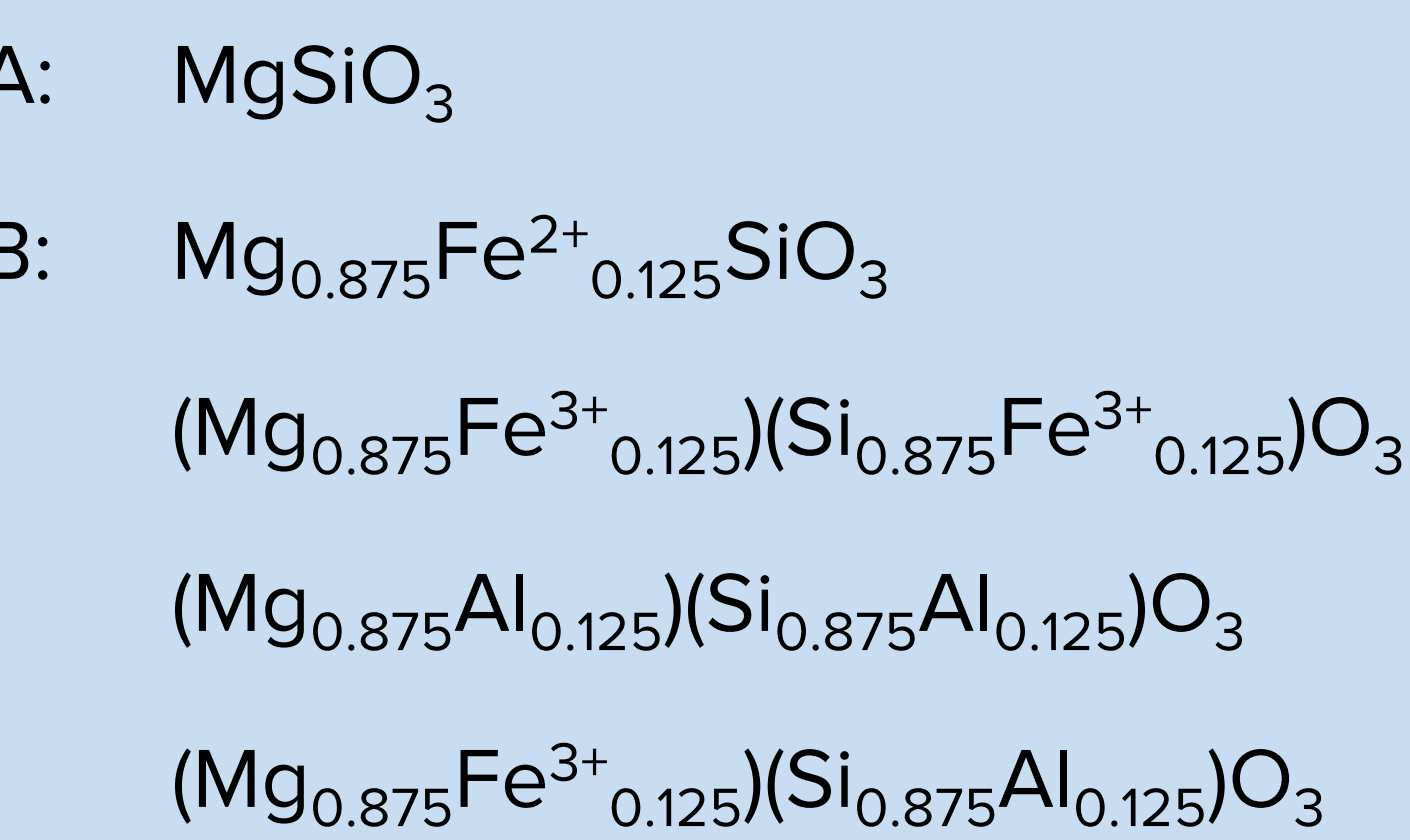


Figure 2. Elastic properties [1,2,3]

Quasi-ideal solid solution model



Gibbs free energy of mixing curves of the Pv and PPv states in a A-B binary system:

$$\Delta G_M^{Pv} = k_B T (X_B \ln[X_B] + (1 - X_B) \ln[1 - X_B]) + X_B (\Delta G_B^{Pv-PPv})$$

$$\Delta G_M^{PPv} = k_B T (X_B \ln[X_B] + (1 - X_B) \ln[1 - X_B]) + (1 - X_B) (\Delta G_A^{Pv-PPv})$$

The compositions of the Pv and PPv solvus lines

$$X_B^{PPv} = \frac{1 - \exp\left(\frac{G_A^{PPv} - G_A^{Pv}}{k_B T}\right)}{\exp\left(\frac{G_B^{PPv} - G_B^{Pv}}{k_B T}\right) - \exp\left(\frac{G_A^{PPv} - G_A^{Pv}}{k_B T}\right)}$$

$$X_B^{Pv} = X_B^{PPv} \times \exp\left(\frac{G_B^{PPv} - G_B^{Pv}}{k_B T}\right)$$

The PPv fraction, n_{PPv} , is given by the lever rule

$$n_{PPv} = \frac{X_B - X_B^{Pv}}{X_B^{PPv} - X_B^{Pv}}$$

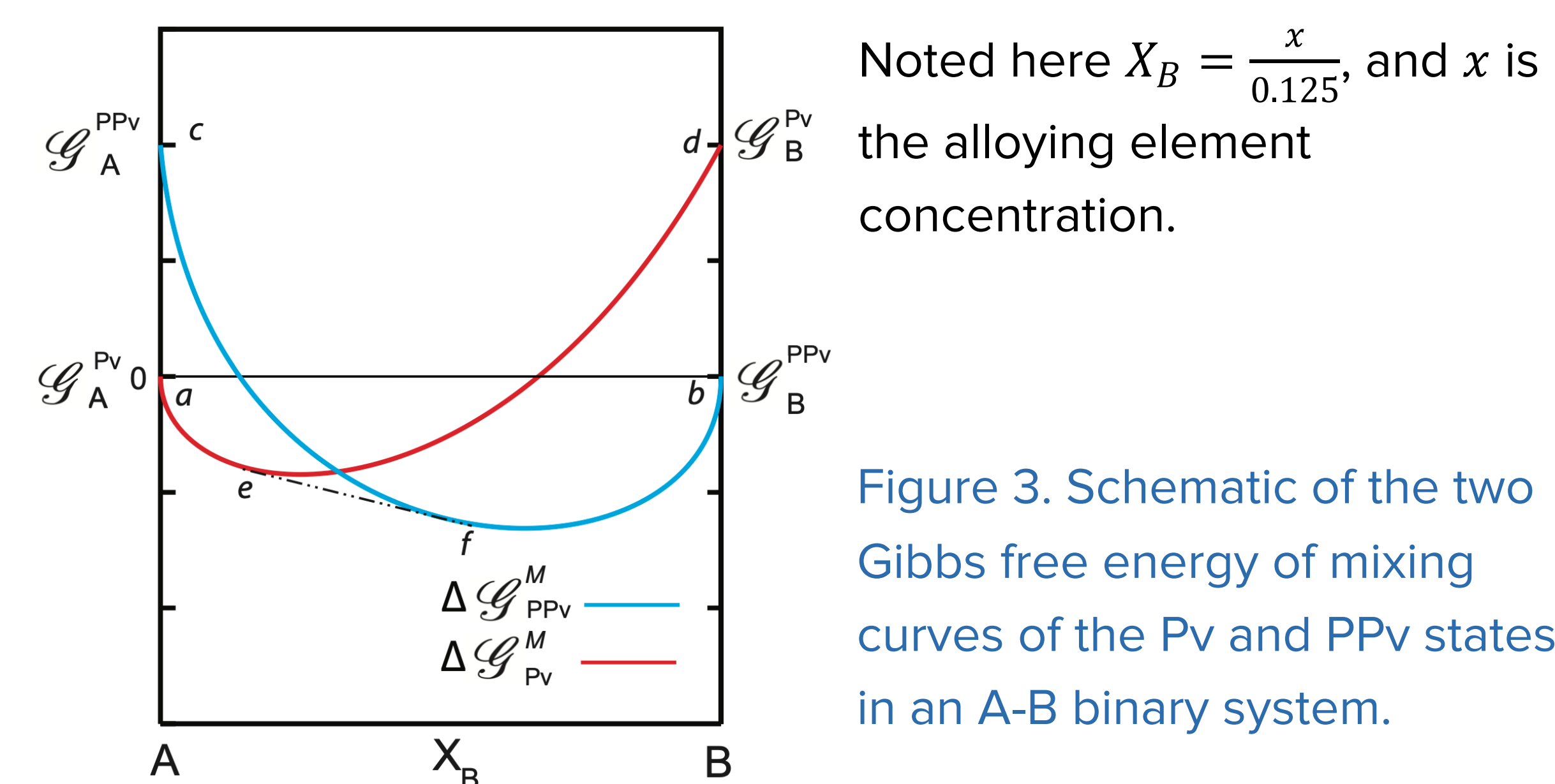


Figure 3. Schematic of the two Gibbs free energy of mixing curves of the Pv and PPv states in an A-B binary system.

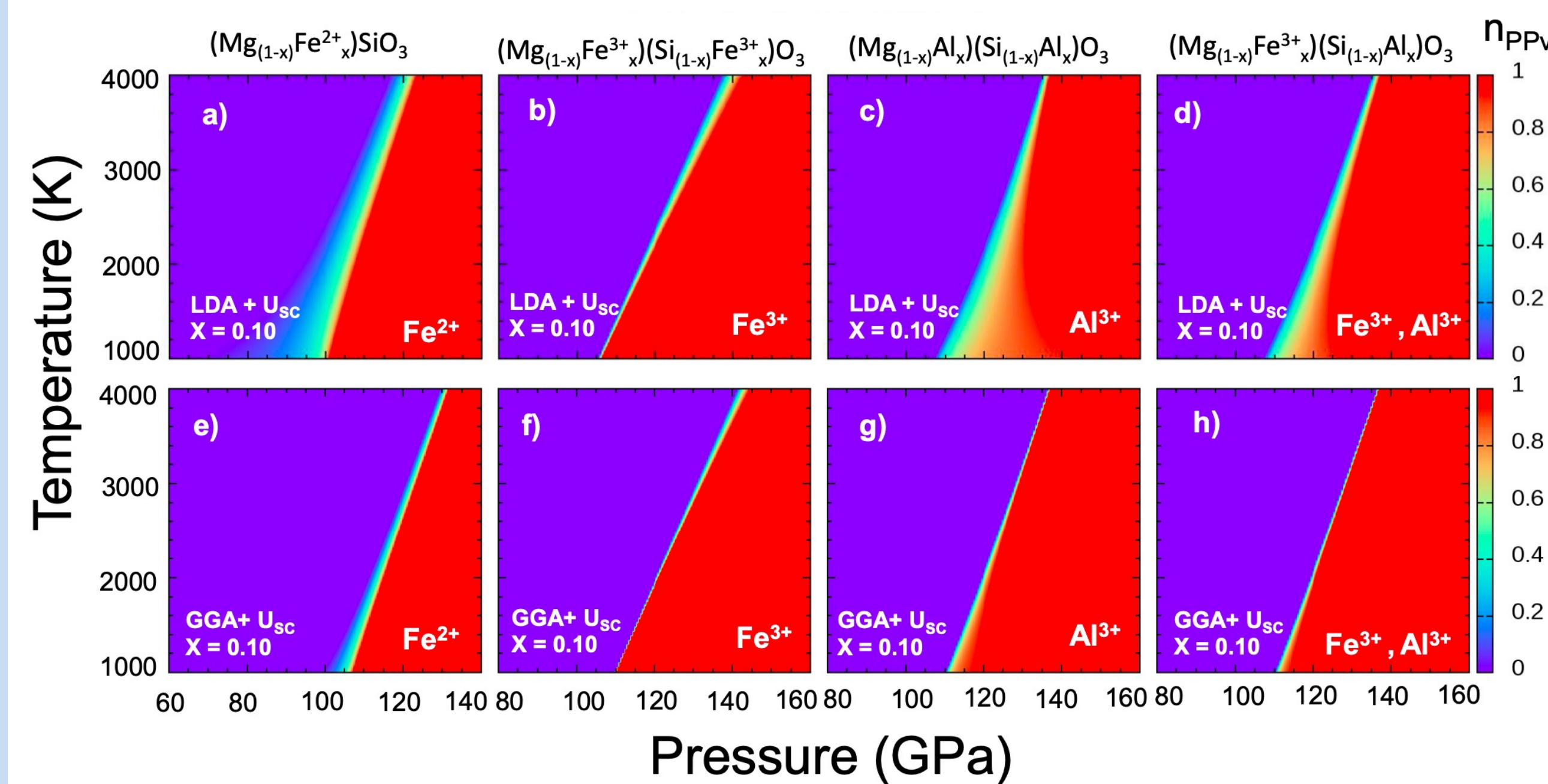
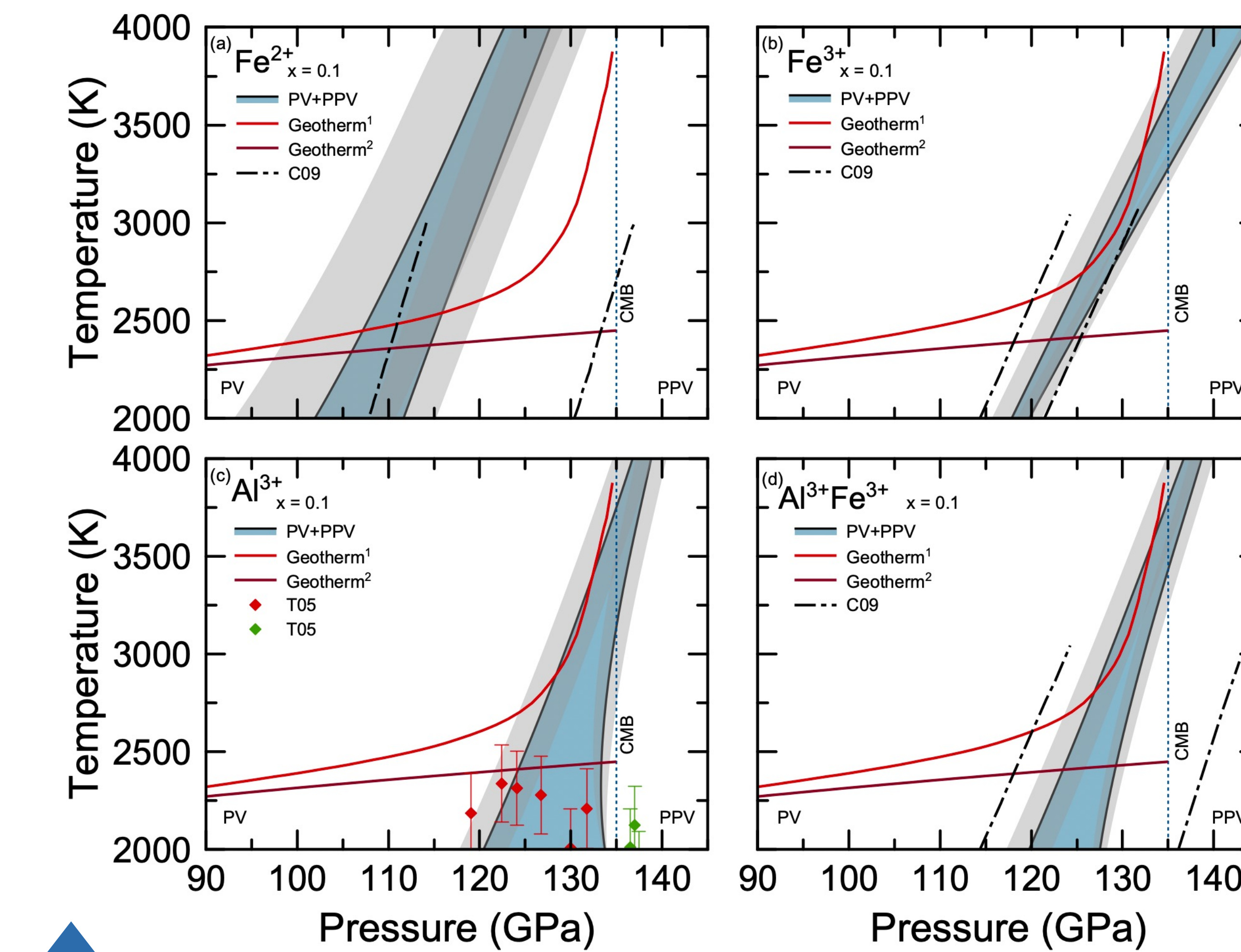


Figure 4. PPv fraction n_{PPv} for all bearing cases, with a bearing element concentration $x=0.10$. The LDA boundaries are generally wider than the GGA boundaries. The differences between the two would result in phase boundary uncertainties.

Pv-PPv Phase boundaries



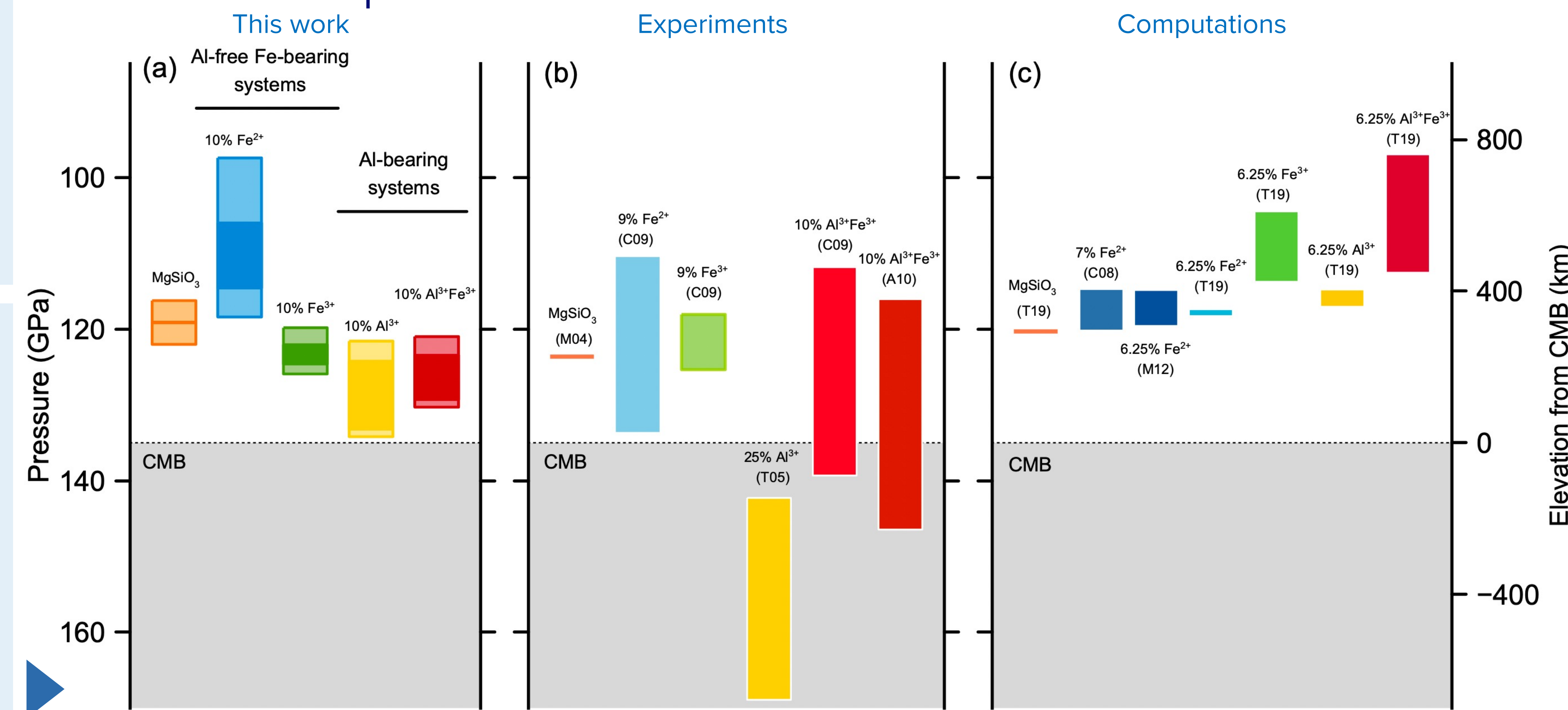
- Blue area shows the coexistence between phases
- Light grey shaded areas are the uncertainties from LDA and GGA data.
- C09 Ref.[5]; T05 Ref.[6]; Geotherm¹ Ref.[7]; Geotherm² Ref.[8].

- The dark colors are the most likely areas of coexistence between the Pv and PPv phases
- The lighter colors are the uncertainties brought by the DFT calculations.
- A10 Ref.[9]; T19 Ref.[10]; C08 Ref.[11]; M12 Ref.[12]

Conclusions

- Fe²⁺ reduces the transition pressure, while Al³⁺, Fe³⁺, (Fe³⁺, Al³⁺)- increase it. The coexistence between Pv and PPv phases grows in proportion to the bearing element concentration.
- The calculated changes in acoustic can serve as a guide to unravel details about the composition of the deep lower mantle.

Depth and thickness of Pv-PPv boundaries



References

- [1] G. Shukla, et al., Geophys. Res. Lett. (2015).
- [2] G. Shukla, et al., Geophys. Res. Lett. (2016).
- [3] G. Shukla, et al., J. Geophys. Res. Solid Earth (2019).
- [4] P. Giannozzi, et al., J. Phys. Condens. Matter (2009).
- [5] K. Catalli, et al., Nature (2005).
- [6] S. Tateno, Geophys. Res. Lett. (2005).
- [7] J. M. Brown and T. J. Shankland, Geophys. J. Int (1981).
- [8] R. Boehler, Rev. Geophys. (2000).
- [9] D. Andrault, et al. Earth Planet. Sci. Lett. (2010).
- [10] X. Wang, et al., Comptes Rendus - Geosci. (2019).
- [11] R. Caracas and R. E. Cohen, Phys. Earth Planet. Inter. (2008).
- [12] A. Metsue and T. Tsuchiya, Geophys. J. Int. (2012).

Acknowledgements

This work is supported by NSF award EAR-1918126 and EAR-2000850, DOE grant DE-SC0019759.

